

# Enhanced Gene Delivery and siRNA Silencing by Gold Nanoparticles Coated with Charge-Reversal Polyelectrolyte

Shutao Guo,<sup>†,‡,§,⊥</sup> Yuanyu Huang,<sup>§,⊥</sup> Qiao Jiang,<sup>†</sup> Yun Sun,<sup>†</sup> Liandong Deng,<sup>‡</sup> Zicai Liang,<sup>§</sup> Quan Du,<sup>§</sup> Jinfeng Xing,<sup>‡</sup> Yuliang Zhao,<sup>†</sup> Paul C. Wang,<sup>†</sup> Anjie Dong,<sup>‡</sup> and Xing-Jie Liang<sup>†,\*</sup>

<sup>†</sup>CAS Key Laboratory for Biomedical Effects of Nanomaterials and Nanosafety, National Center for Nanoscience and Technology of China, Beijing 100190, China, <sup>‡</sup>School of Chemical Engineering and Technology, and School of Material Science and Engineering, Tianjin University, Tianjin 300072, China, and <sup>§</sup>Laboratory of Nucleic Acid Technology, Institute of Molecular Medicine, Peking University, Beijing 100871, China. <sup>⊥</sup>These authors contributed equally to this work.

Over the past decade, due to good biocompatibility, easy synthesis, monodispersity, and ready functionalization, gold nanoparticles have emerged as an attractive candidate for delivery of various payloads into cells, such as small drug molecules or large biomolecules,<sup>1–5</sup> such as DNA and siRNA.<sup>6–13</sup> The intracellular release could be triggered by glutathione (GSH),<sup>3</sup> pH, or external (e.g., light) stimuli.<sup>1,4,14–17</sup> siRNA has emerged recently as a promising method for biological research and holds great potential for treatment of human diseases.<sup>18–20</sup> Nucleic acid was mostly loaded by gold nanoparticles through thiol linkages or electrostatic interaction with cationic gold nanoparticles.<sup>6–13,21,22</sup> Elbakry *et al.* first developed the PEI/siRNA/PEI-AuNP system to deliver siRNA into cells and knockdown the expression of target gene based on the self-assembly layer-by-layer technology.<sup>11</sup> PEI, which has strong escape capacity from the endosome due to its so-called “proton sponge” effect and is usually a gold standard of polymeric transfection agent, was deposited on the gold nanoparticles to bind siRNA. However, the release extent of siRNA in cellular cytoplasm was low, due to the high binding ability between the gold nanoparticles and siRNA. Therefore, to achieve the same knockdown efficacy of gene expression with the PEI/siRNA system, more amounts of siRNA and PEI are usually needed for the PEI/siRNA/PEI-AuNP system.

It is believed that successful escape of siRNA carriers from endosome and release of the payload into cytoplasm, where siRNA plays a function, are prerequisites for improving the gene silencing. For polymeric plas-

**ABSTRACT** Charge-reversal functional gold nanoparticles first prepared by layer-by-layer technique were employed to deliver small interfering RNA (siRNA) and plasmid DNA into cancer cells. Polyacrylamide gel electrophoresis measurements of siRNA confirmed the occurrence of the charge-reversal property of functional gold nanoparticles. The expression efficiency of enhanced green fluorescent protein (EGFP) was improved by adjuvant transfection with charge-reversal functional gold nanoparticles, which also had much lower toxicity to cell proliferation. Lamin A/C, an important nuclear envelope protein, was effectively silenced by lamin A/C-siRNA delivered by charge-reversal functional gold nanoparticles, whose knockdown efficiency was better than that of commercial Lipofectamine 2000. Confocal laser scanning microscopic images indicated that there was more cy5-siRNA distributed throughout the cytoplasm for cyanine 5-siRNA/polyethyleneimine/*cis*-aconitic anhydride-functionalized poly(allylamine)/polyethyleneimine/11-mercaptopoundecanoic acid-gold nanoparticle (cy5-siRNA/PEI/PAH-Cit/PEI/MUA-AuNP) complexes. These results demonstrate the feasibility of using charge-reversal functional gold nanoparticles as a means of improving the nucleic acid delivery efficiency.

**KEYWORDS:** gold nanoparticles · charge-reversal polyelectrolyte · drug delivery · layer-by-layer assembly · siRNA delivery

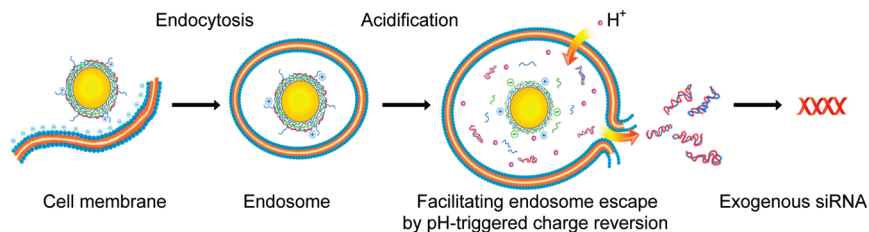
mid delivery, to improve the efficiency of intracellular delivery and release of the nucleic acid (DNA or siRNA), ternary complexes composed of nucleic acid, polycations, and a charge-reversal polymer were developed. Charge-reversal copolymer is a kind of copolymer that could pH-dependently shift charge nature between positive and negative. The charge-reversal copolymers are usually used to improve the gene delivery efficiency by enhancing endosome escape capacity.<sup>10,23–26</sup> When the vector (ternary complexes) is entrapped into the acidic intracellular organelles such as endosome or lysosome ( $\text{pH} = 5–6$ ), charge conversion would facilitate the endosomal escape of the polyplexes through membrane disruption by enhancing the capacity of “proton sponge”. Charge-reversal polymers are important for improving the efficiency of transfection. So far, no ideal vectors have been developed to utilize gold nanoparticles and charge-reversal

\*Address correspondence to liangxj@nanoctr.cn.

Received for review July 14, 2010 and accepted August 06, 2010.

Published online August 13, 2010. 10.1021/nm101638u

© 2010 American Chemical Society



**Scheme 1.** Enhanced intracellular payload release at endosome by pH-dependent charge-reversal polyelectrolyte on gold nanoparticles.

polymers to deliver and release drugs or nucleic acids *in vitro* and *in vivo*. Indeed, the multifunctional vectors can be obtained by depositing opposite charged polyelectrolytes with functional molecules on gold nanoparticles.<sup>27</sup> Charge-reversal polyelectrolyte-deposited gold nanoparticles have several unique properties, such as disrupting the endosome efficiently, releasing pharmaceutical agents easily, and versatile modification by polyelectrolyte-bearing nonbiofouling poly(ethylene glycol) (PEG) or target ligands (as shown in Scheme 1).

In this work, charge-reversal PEI/PAH-Cit/PEI/MUA-AuNPs were prepared with cationic PEI, charge-reversal PAH-Cit, and MUA-AuNPs by layer-by-layer assembly technique (as shown in Figure S1 in the Supporting Information) as nucleic acid carriers. It has confirmed that the charge reversion of PAH-Cit does work in the siRNA/PEI/PAH-Cit/PEI/MUA-AuNP system after changing pH values from 7.4 to 5.0 by polyacrylamide gel electrophoresis (PAGE). In addition, gene transfection and siRNA knockdown studies *in vitro* show high efficiency of the payload release due to the charge reversion of PAH-Cit. Compared to the commercial transfection agents Lipofectamine and PEI, charge-reversal PEI/PAH-Cit/PEI/MUA-AuNP present higher efficiency at the same amount of siRNA. This is the first study demonstrating that charge-reversal process was easily confirmed by the layer-by-layer technology on the nanoparticles and very effective to enhance the gene transfection and siRNA knockdown efficiency.

## RESULTS AND DISCUSSION

**Synthesis and Characterization of Gold Nanoparticles Coated with Charge-Reversal Polymer.** Spherical gold nanoparticles with the size of 15 nm determined by TEM (Figure S2, Supporting Information) were synthesized. To facilitate

the polyelectrolyte deposition on the gold nanoparticles, original citrate–gold nanoparticles were chemically modified by MUA. Cationic polymers, such as PEI, poly-L-lysine (PLL), and chitosan, can form complexes with nucleic acid through electrostatic interactions and are used to be polymeric gene transfection materials as promising alternatives of viral vectors. Among them, PEI is the gold standard for gene delivery, which has strong escape capacity from endosome due to “proton sponge” effect. In the past, a lot of work had been done on improving the gene transfection efficiency based on PEI. PEI was selected as a polyelectrolyte to be deposited or bonded on the surface of gold nanoparticles. PAH-Cit, one kind of charge-reversal polymer, was first synthesized by Lynn *et al.* and successfully used to fabricate polyelectrolyte multilayers.<sup>26</sup> The authors confirmed the occurrence of charge-reversal property by determining the thickness of the film and the remaining of amide bond by <sup>1</sup>H NMR. Therefore, PEI and PAH-Cit were used as opposite polyelectrolytes to modify gold nanoparticles in this study to improve gene transfection and gene silencing efficiency.

The process of polyelectrolyte deposition on gold nanoparticles was monitored by measurement of zeta potential with dynamic light scattering (DLS), UV–vis absorbance spectra, and TEM. Measurement of reversal zeta potential indicated the successful deposition of polyelectrolyte after each of coating step (Figure 1A). The peak of plasmon absorbance ( $\lambda_{\text{max}}$ ) in UV–vis spectra (Figure 1B) was found to shift from 523 to 526 nm after all of the layers deposited at pH 7.4, whereas no broadening in the peak plasmon absorbance of the gold nanoparticles occurred after deposition of polyelectrolytes, indicating gold nanoparticles remained dispersed. This was further confirmed by the images of

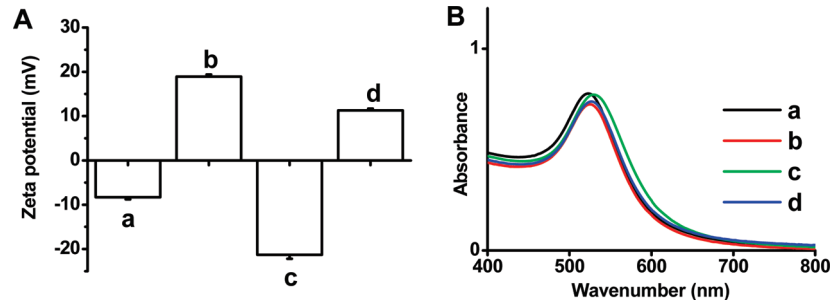


**Figure 1.** Zeta-potential of colloidal AuNPs (A) and UV–vis spectra of MUA-AuNPs (a), PEI/MUA-AuNPs (b), PAH-Cit/PEI/MUA-AuNPs (c), and PEI/PAH-Cit/PEI/MUA-AuNPs (d) in 10 mM HEPES buffer at pH 7.4 (B).

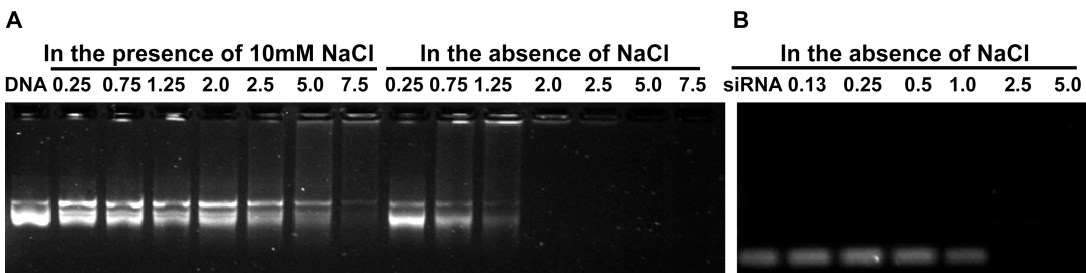


**Figure 2.** Agarose gel electrophoresis retardation assay of DNA/PEI/PAH-Cit/PEI/MUA-AuNP (A) and siRNA/PEI/PAH-Cit/PEI/MUA-AuNP (B) complexes at different w/w ratios of Au to nucleic acid. The numbers denote the ratio.

TEM (Figure S2, Supporting Information). These results demonstrate that most of particles remain dispersed after deposition of polyelectrolytes, and optimal nanoparticles used for loading nucleic acid were obtained.

During the process of layer deposition, to get the uniform PAH-Cit/PEI/MUA-AuNPs, its preparation was done in the presence of 10 mM NaCl (as shown in Figure S1, Supporting Information). It is known that the salt concentration would affect the conformation of polyelectrolyte,<sup>28,29</sup> which exhibits flat conformation in water and loops or tails conformation in the presence of salt. Therefore, the condition for layer deposition is carefully established to enable PEI/PAH-Cit/PEI/MUA-AuNPs with high ability to bind nucleic acid. Deposition of PEI on the PAH-Cit/PEI/MUA-AuNPs was done in the presence of 10 mM NaCl or no NaCl. The agarose gel retardation assay indicated that complete retardation of plasmid DNA and siRNA in the absence of salt was achieved at the w/w ratios of 2 and 2.5, respectively. The different ability to condense DNA and siRNA was related to different molecular weight of nucleic acid. However, complete retardation of plasmid DNA was achieved above the w/w ratios of 7.5 in the presence of 10 mM NaCl (Figure 2). Therefore, at the last step, preparation of PEI/PAH-Cit/PEI/MUA-AuNPs was performed in the absence of salt (Figure S1, Supporting Information).

#### Confirm the Charge-Reversal Process of PAH-Cit on Gold Nanoparticles.

**Nanoparticles.** It was hypothesized that the charge-reversal polymers could improve the release of nucleic acid off the gold nanoparticles and enhance the proton sponge effect. These unique polymers were often used in the formation of multilayer film or ternary complexes to release pharmaceutical agents in drug delivery systems triggered by pH stimuli degradation, and the process of charge reversion was usually traced by the thickness of film or the reversal of zeta potential.<sup>10,26</sup> The layer number of films was up to 20, and charge reversion of PAH-Cit was also confirmed by determining the thickness of the film and the remaining of amide bond by <sup>1</sup>H NMR, which indicated that the hydrolysis of PAH-Cit was not blocked. Because of the difficulty of fabricating nanoparticle complexes and the limited sample amount, we took another method to trace the charge reversion process of PAH-Cit using gel electrophoresis technology. To verify the charge reversion process, poly(styrenesulfonate) (PSS) was used as a control. It is

assumed that the charge reversion reaction would occur at pH 5.0 for siRNA/PEI/PAH-Cit/PEI/MUA-AuNPs. With occurrence of the charge-reversal process, siRNA, the outer PEI, and partially hydrolyzable PAH-Cit would be released off the gold nanoparticles. After treated by acid for different times, the supernatant of siRNA/PEI/PAH-Cit/PEI/MUA-AuNPs and siRNA/PEI/PSS/PEI/MUA-AuNPs was separated. Heparin was used to obtain free siRNA from the supernatant mixture. Then, PAGE of siRNA was performed to determine the amount of siRNA released due to charge reversion. As a result, more siRNA was released with increasing incubation time at pH 5.0 for siRNA/PEI/PAH-Cit/PEI/MUA-AuNPs (as shown in Figure 3A). However, significantly reduced siRNA was observed for siRNA/PEI/PSS/PEI/MUA-AuNP control group at same condition. Only a negligible siRNA amount, which is residual siRNA due to the incomplete centrifuge, was detected for all samples treated with pH 7.4 buffer (as shown in Figure 3B). Therefore, it is concluded that PAH-Cit polyanion indeed undergoes the charge-reversal reaction and is very helpful at releasing siRNA, which may facilitate improved gene transfection and gene silencing efficiency.

#### DNA Transfection Efficiency and siRNA Silencing Efficiency.

The transfection efficiency of PEI/PAH-Cit/PEI/MUA-AuNPs was studied by performing GFP and luciferase protein expression experiments with HeLa cells at a variety of w/w ratios. PEI and Lipofectamine 2000 were used as positive controls. To eliminate multivalency effects assisted by AuNPs and demonstrate the charge-reversal effect, PEI/MUA-AuNPs and PEI/PSS/PEI/MUA-

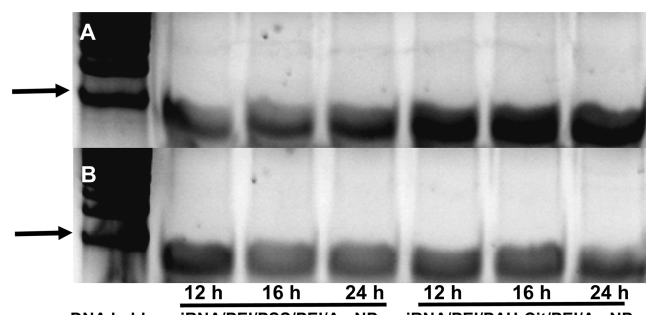


**Figure 3.** Polyacrylamide gel electrophoresis for siRNA/PEI/PSS/PEI/Au NPs and siRNA/PEI/PAH-Cit/PEI/Au NPs after treated with pH 5.0 acetic buffer (A) and pH 7.4 HEPES buffer (B). Left lane is 20 bp DNA ladder, and the arrow marks the band of 40 bp.

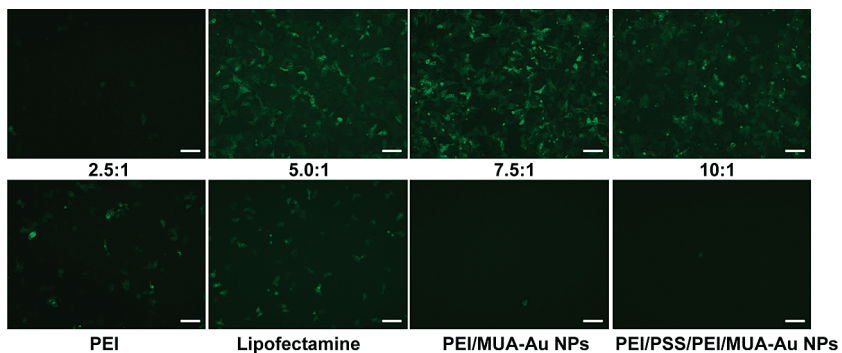


**Figure 4.** HeLa cells were transfected with DNA/PEI/PAH-Cit/PEI/MUA-AuNP complexes. The transfection was performed at various w/w ratios of Au/DNA (top panel). Lipofectamine, PEI/MUA-AuNP, PEI/PSS/PEI/MUA-AuNP, and PEI/DNA ( $N/P = 10$ ) complexes were used as control (bottom panel). The w/w ratio of Au/DNA 7.5 was used for PEI/MUA-AuNPs and PEI/PSS/PEI/MUA-AuNPs. The scale bar is  $30 \mu\text{m}$ .

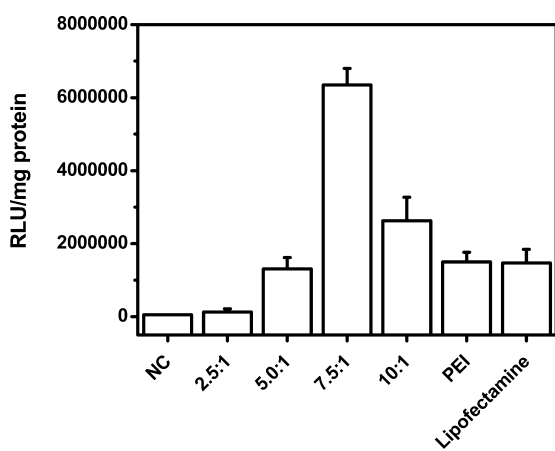


**Figure 5.** *In vitro* transfection efficiency of DNA/PEI/PAH-Cit/PEI/MUA-AuNP complexes at different ratios by luciferase assay on the HeLa cell line. Lipofectamine and PEI ( $N/P = 10$ ) were used as positive controls.

AuNPs were also used as controls, respectively. As shown in Figure 4, at the w/w ratio of Au/DNA 7.5, the most efficient transfection was obtained for DNA/PEI/PAH-Cit/PEI/MUA-AuNP complexes. At the ratio of Au/DNA 10, transfection efficiency was reduced, whereas at lower ratio, only a few transfected cells can be detected. For PEI/MUA-AuNPs and PEI/PSS/PEI/MUA-

AuNPs, their transfection efficiency was low at the optimal ratio of 7.5 as was PEI/PAH-Cit/PEI/MUA-AuNPs. In addition, we also examined gene transfection efficiency of PEI/PAH-Cit/PEI/MUA-AuNPs on HEK 293T cells. PEI/PAH-Cit/PEI/MUA-AuNPs also exhibit positive results (as shown in Figure S3, Supporting Information). It clearly indicates that GFP expression is better in charge-reversal PEI/PAH-Cit/PEI/MUA-AuNPs than that in PEI/PSS/PEI/MUA-AuNPs and PEI, thereby their potential as a gene carrier and the charge-reversal PAH-Cit may play an important role in improving efficiency of gene therapy.

Next, the gene transfection efficiency was also confirmed at protein expression level by using the pGL3.0 plasmid. As shown in Figure 5, the result is in accordance with that obtained from the EGFP-N1 transfection experiment. PEI/PAH-Cit/PEI/MUA-AuNPs presented best transfection efficiency at the optimal ratio of 7.5. At the ratio of 7.5, luciferase expression levels for PEI/PAH-Cit/PEI/MUA-AuNPs were 3.2- and 3.3-fold higher than those of PEI ( $N/P = 10$ ) and Lipofectamine 2000 as positive controls in the HeLa cell line, respectively.

To further evaluate the silencing efficiency of siRNA delivered by PEI/PAH-Cit/PEI/MUA-AuNPs, the suppression of an endogenous protein, lamin A/C, was examined in HeLa cells. Lamin A/C encoded by LMNA gene, an important component of the nuclear envelope, consists of a two-dimensional matrix of proteins located next to the cellular inner nuclear membrane. Lamin A/C proteins are thought to be involved in nuclear stability, chromatin structure, and gene expression. Depolymerization of the nuclear lamin A/C leads to disintegration of the nuclear envelope. Defects in the lamin A/C gene (LMNA) have been associated with a variety of pathologies, affecting mainly muscular, autosomal recessive CMT2, and adipose tissues.<sup>30</sup> The siRNA transfection experiment was designed the same as the EGFP plasmid transfection experiment. Down regulation of the lamin A/C protein expression was examined by Western blot. The experiments were carried out with 1  $\mu\text{g}$  of siRNA at different ratios. After 48 h, the cells were

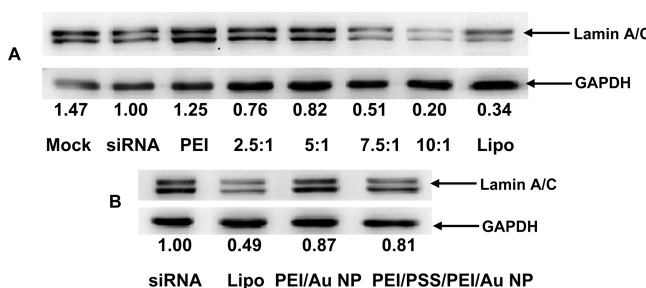


**Figure 6.** Knockdown of lamin A/C expression was determined by Western blot over 48 h in HeLa cells using lamin A/C-siRNA delivered by PEI/PAH-Cit/PEI/MUA-AuNPs at various ratios (A); Lipofectamine 2000 (Lipo), PEI (at the  $N/P$  ratio of 10), PEI/AuNPs, and PEI/PSS/PEI/AuNPs (at the Au/siRNA ratio of 10) were used as controls (B). The data of panels A and B were done in different experiments. GADPH was used as the internal standard for Western blot. The numbers under the images denote the ratio of lamin A/C protein expression to that in the siRNA group, which is set as internal reference = 1.00.

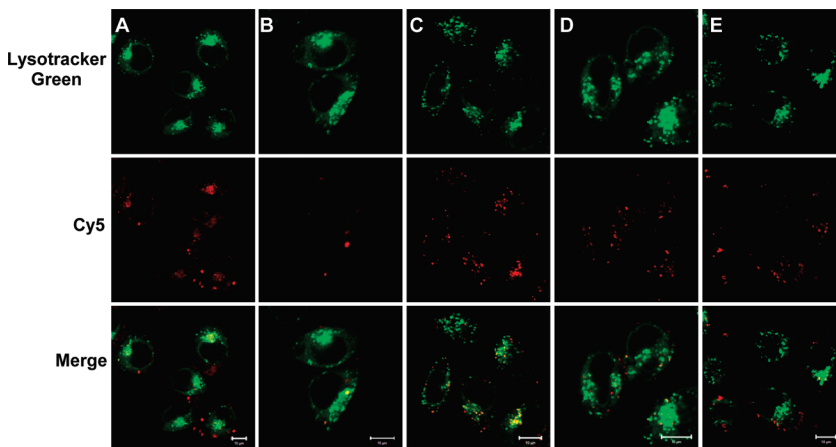


**Figure 7.** CLSM images of HeLa cells transfected by PEI/PAH-Cit/PEI/MUA-AuNPs (A), Lipofectamine (B), PEI (C), PEI/MUA-AuNPs (D), and PEI/PSS/PEI/MUA-AuNPs (E). The w/w ratio of Au/DNA 10.0 was used for all of the gold nanoparticles. Images were taken after cells were incubated with NPs for 6 h. siRNA was labeled with cy5 (red, middle row). The late endosome and lysosome were stained with LysoTracker Green (green, first row). The yellow fluorescence (third row) is a result of colocalization of LysoTracker Green and cy5-labeled siRNA. The scale bar is 10  $\mu\text{m}$ .

lysed and assayed for Western blot. The results are shown in Figure 6. Quantification of lamin A/C protein expression indicated that the knockdown efficiency of siRNA delivered by PEI/PAH-Cit/PEI/MUA-AuNPs was dose-dependent. Lamin A/C-siRNA delivered by PEI/PAH-Cit/PEI/MUA-AuNPs at the ratio of Au/DNA 10 showed most significant inhibition of lamin A/C expression in HeLa cells and resulted with 80.0% knockdown efficiency, which was higher than 66.0% knockdown efficiency of cells delivered by Lipofectamine 2000. Similar to GFP expression assay, it is not strange that PEI/AuNPs and PEI/PSS/PEI/AuNPs are less effective in knockdown of lamin A/C expression. Thus, these results demonstrate that the charge-reversal PAH-Cit may play an important role in releasing siRNA to improve siRNA silencing, compared to the previous research.<sup>11</sup>

**Cellular Internalization and Distribution.** It is known that the successful escape from endosomes is crucial for siRNA carriers to improve siRNA silencing efficiency. The penetration ability of cy5-siRNA/PEI/PAH-Cit/PEI/MUA-AuNP complexes into cells was investigated by confocal laser scanning microscopy (Figure 7). Images were taken to measure fluorescence in HeLa cells after transfection for 6 h. LysoTracker Green is a fluorescent acidotropic probe for labeling and tracking acidic organelles in live cells, such as lysosome and endosome. As shown in Figure 7, it is interesting to note that, for cy5-siRNA/PEI/PAH-Cit/PEI/MUA-AuNP complexes, more cy5-siRNA was distributed over the cytoplasm. However, the formed complexes for siRNA and Lipofectamine 2000 or PEI were likely to be tightly clustered

in punctate structures rather than distributed over the cytoplasm. It is demonstrated that the release of siRNA delivered by PEI/PAH-Cit/PEI/MUA-AuNPs is more efficient after being delivered inside the cells, which may be deduced by the charge reversion of PAH-Cit. It is known that localization into cytoplasm is the critical prerequisite of siRNA delivery to effectively silence specific mRNA. In addition, cell viabilities assayed by MTT indicated that gold nanoparticles were almost nontoxic to cells (Figure S4, Supporting Information).

## CONCLUSION

To our knowledge, this is the first report of charge-reversal polyelectrolyte deposited gold nanoparticles as carrier for gene delivery. These novel gold nanoparticles can both effectively enhance gene delivery efficiency and regulate gene expression in the context of RNA interference, suggesting the charge reversion under acidic environment facilitates the escape of gold nanoparticle/nucleic acid complexes from endosome/lysosome and release of functional nucleic acids into cytoplasm. Significantly, the layer-by-layer technique could be successfully used to form multifunctional gold nanoparticles for therapeutic applications. After the surface of PEI/PAH-Cit/PEI/AuNPs was coated by a layer of polyelectrolyte bearing PEG and ligand moieties, the blood circulation time of PEI/PAH-Cit/PEI/AuNPs and the bioavailability of drugs would be improved. These nanoparticles may be very promising to deliver nucleic acid for *in vivo* therapeutic applications.

## MATERIALS AND METHODS

**Materials.** Branched PEI ( $M_w = 25$  kDa), PSS ( $M_w = 70$  kDa), PAH ( $M_w = 15$  kDa), and MUA were purchased from Sigma-Aldrich (St Louis, MO). PAH-Cit was synthesized by the reported procedure.<sup>26</sup> Tetrachloroauric(III) acid and sodium citrate were

obtained from Sinopharm (Shanghai, China). EGFP-N1 plasmid was amplified in *Escherichia coli* of DH5 $\alpha$  and purified by column chromatography, which can remove endotoxins (QIAGEN-Mega Kit, QIAGEN, Chatsworth, CA). Dulbecco's modified Eagle's medium (DMEM) and fetal bovine serum (FBS) were purchased from

Invitrogen Corporation (Carlsbad, CA). Ethidium bromide, dimethyl sulfoxide (DMSO), and 3-[4,5-dimethylthiazol-2-yl]-2,5-diphenyltetrazolium bromide (MTT) were purchased from Sigma-Aldrich (St Louis, MO). Agarose was purchased from GEN TECH (Hong Kong, China). Cy5-labeled siRNA was purchased from Guang Zhou Ribobio Co., Ltd. (Guangzhou, Guangdong Province, China), and the sequences were as follows: sense strand, 5'-UCUCUCCGAACGUGUCACGUdTdT-3'; antisense strand, 5'-ACGUGACACGUUCGGAGAAdTdT-3'. Cy5 fluorophore was labeled at 5' of the sense strand. siRNA used for silence lamin A/C gene was purchased from Shanghai GenePharma Co., Ltd. (Shanghai, China), and the sequences were as follows: sense strand, 5'-CUGGACUUCAGAACAdTdT-3'; antisense strand, 5'-UGUUCUUCUGGAAGUCCAGdTdT-3'.

**Preparation of MUA-AuNPs.** MUA-AuNPs were prepared as described previously.<sup>11</sup> Briefly, 2.0 mL of 1%  $\text{AuCl}_4 \cdot 3\text{H}_2\text{O}$  solution was added into 200 mL of double-distilled water and heated under reflux until boiling. Then, 5.0 mL of a 1% trisodium citrate solution were added under vigorous stirring. Boiling was continued for 10 min. The larger aggregates were removed by filtration using 220 nm filters. The pH of AuNPs was adjusted to 11, followed by the addition of MUA at a final concentration of 0.1 mg/mL. The reaction was performed at room temperature for 24 h. The stabilized particles were purified twice at 15 200g for 15 min and stocked in 1 mM NaCl.

**Preparation of Polyelectrolyte-Coated MUA-AuNP Complexes Loaded with/without DNA or siRNA.** For each deposition step, to prepare PEI/MUA-AuNPs, PAH-Cit/PEI/MUA-AuNPs, and PEI/PAH-Cit/PEI/MUA-AuNPs, the concentration of polyelectrolyte was fixed at 1.0 mg/mL. Each coating step was performed for 30 min after the addition of the gold nanoparticles to the respective stirring polyelectrolyte solution. Purification of the crude AuNPs was performed twice at 15 200g for 20 min, and the AuNPs were resuspended in 10 mM HEPES buffer (pH 7.4). At the last step, 1.0 mL of PEI/PAH-Cit/PEI/MUA-AuNPs was condensed into 50  $\mu\text{L}$  solution.

The diluted nucleic acid solutions (20  $\mu\text{g}/\text{mL}$  in 10 mM HEPES buffer) were combined with PEI/PAH-Cit/PEI/MUA-AuNPs with the w/w ratio (which is defined as the ratio between Au and nucleic acid). The resulting mixtures were mixed by pipetting and incubated for 20 min at room temperature before further operation. PEI/MUA-AuNPs, PEI/PSS/PEI/MUA-AuNPs, and their complexes with DNA or siRNA were prepared similarly.

**Charge Reversion Assay of siRNA/PEI/PAH-Cit/PEI/MUA-AuNPs.** Experiments designed to confirm the charge reversion of PAH-Cit layer were performed in the following procedure: 35  $\mu\text{L}$  well incubated siRNA/PEI/PAH-Cit/PEI/MUA-AuNPs (at the Au/siRNA ratio of 7.5) were diluted by 75  $\mu\text{L}$  0.2 M acetic buffer (pH 5.0) or 0.02 M HEPES buffer (pH 7.4). After incubation for different time intervals, the mixture was centrifuged at 14 000 rpm for 15 min. Five microliters of heparin solution (60  $\mu\text{g}/\text{mL}$ ) was added into the supernatant to release siRNA off the complexes formed by siRNA and PEI or partially hydrolyzed PAH-Cit. The amount of siRNA in supernatant was analyzed by PAGE. Twenty microliters of siRNA solution was mixed with 5  $\mu\text{L}$  of 6 $\times$  loading buffer (Takara Biotechnology Co, Dalian, Liaoning Province, China) and then loaded onto 20% polyacrylamide gel. Electrophoresis was carried out at a voltage of 120 V for 1.5 h in 2 $\times$  TBE running buffer. Then the gel was stained in 2 $\times$  TBE buffer, which contains 1 $\times$  SYBR gold nucleic acid gel stain (Invitrogen, USA) for 20 min. Finally, the results were recorded using gel imaging system (Vilber Lourmat, France).

**Nanoparticle Characterization.** Electron micrographs were obtained with a transmission electron microscope (TEM) (Tecnai G2 20 S-TWIN, FEI Company, Hillsboro, OR). Samples were prepared by depositing 7.5  $\mu\text{L}$  of colloidal gold solution onto a carbon-coated copper grid and air-dried before analysis. UV-visible spectra were recorded on a Lambda 950UV/vis/NIR spectrophotometer in the range of 400–800 nm. Zeta potential was determined on a Nano-ZS (Malvern, Worcestershire, UK) zetasizer at a scattering angle of 173° and analyzed using the DTS (Nano) program. Three measurements (each with 20 subruns) were performed for each sample.

**Agarose Gel Electrophoresis.** The agarose gel retardation assay was performed as follows: 20  $\mu\text{L}$  well incubated DNA/PEI/PAH-

Cit/PEI/MUA-AuNP complexes solution was mixed with 4  $\mu\text{L}$  of 6 $\times$  loading buffer (Takara Biotechnology, Dalian, Liaoning Province, China), and then 20  $\mu\text{L}$  of the mixture was loaded onto 1% agarose gel (2% for siRNA) containing 0.5  $\mu\text{g}/\text{mL}$  ethidium bromide (5.0  $\mu\text{g}/\text{mL}$  for siRNA). Electrophoresis was carried out at a voltage of 110 V for 40 min in 1 $\times$  TAE running buffer (120 V, 15 min for siRNA). Finally, the results were recorded at UV light wavelength of 254 nm by Typhoon Trio (GE Healthcare, Salt Lake City, UT).

**Plasmid Transfection.** HeLa cells were seeded in 24-well plates at  $0.5 \times 10^5$  cells per well and incubated in DMEM supplemented with 10% FBS, 100 U/mL penicillin, and 100 mg/mL streptomycin for 20 h before transfection. Then the medium was removed and replaced by serum-free DMEM. Subsequently, DNA/PEI/PAH-Cit/PEI/MUA-AuNP complexes containing 1  $\mu\text{g}$  of EGFP-N1 plasmid were added into each well. After 4 h incubation at 37 °C in 5% CO<sub>2</sub> humidified atmosphere, the transfection solutions were aspirated and substituted by complete culture medium. After additional 36 h incubation, the cells were directly observed by an inverted microscope (Olympus IX 70, Olympus, Tokyo, Japan). The microscopy images were obtained at the magnification of 40 $\times$  and recorded using Cool SNAP-Pro (4.5.1.1) software.

The pGL3.0 plasmid was further used to evaluate the transfection efficiency, and Lipofectamine and branched PEI ( $M_w = 25$  kDa) were used as the positive controls. Transfection experiment was performed as before. After 36 h incubation, the medium was removed and cells were washed twice by PBS, then the cells were lysed using 200  $\mu\text{L}$  of 1 $\times$  reporter lysis buffer (Promega Co., Madison, WI) followed by freeze–thaw cycles to ensure complete lysis. The cell lysate was transferred into a 1 mL centrifuge vial and centrifuged for 30 s at 12 000 rpm, and the supernatant was collected for luminescence measurements. The relative light units (RLUs) were measured with a fluorometer (Synergy HT, BioTek, USA). The total protein was measured according to a BCA protein assay kit (Pierce, Rockford, IL), and gene transfection efficiency is presented as RLU/mg protein.

**Cytotoxicity by MTT Assay.** The cells were seeded in 96-well plates at  $1 \times 10^4$  cells per well and subsequently transfected using similar protocol as described above. After 24 h incubation, 20  $\mu\text{L}$  of MTT solutions (5 mg/mL in PBS) was added to each well and incubated at 37 °C in 5% CO<sub>2</sub> for 4 h. Then solution in the wells was aspirated gently and 150  $\mu\text{L}$  of DMSO was added into each well to dissolve the formazan crystals. After shaking for 10 min, the absorbance of each well at 490 nm was measured by Infinite M200 (TECAN, Männedorf, Switzerland). The results were expressed as the mean percentage of cell viability relative to untreated cells.

**Uptake of PEI/PAH-Cit/PEI/MUA-AuNP/siRNA Complexes.** For cell uptake studies, HeLa cells were plated in 6-well plates with a glass coverslip at the bottom with  $2 \times 10^5$  cells per well one day before transfection. Cy5-siRNA/PEI/PAH-Cit/PEI/MUA-AuNPs at the w/w ratio of Au/siRNA 10 were transfected to the cell as the procedure above. Six hours later, distributions of the nucleic acids were examined and recorded in living cells by using Zeiss confocal microscopy (LSM700, Carl Zeiss Shanghai Co. Ltd., Shanghai, China). Meanwhile, Lysotracker Green DND-26 (Invitrogen, Carlsbad, CA) was used to indicate the endosome/lysosome organelles. Imaging processing programs were coded in Interactive Data Language.

**Gene Silencing Efficiency Evaluated by Western Blotting.** For gene silencing experiments, HeLa cells were plated in 6-well plates at  $2 \times 10^5$  cells per well one day before transfection. siRNA transfection was carried as described above on the next day. Forty-eight hours later, protein was collected and the concentration was measured with BCA protein assay kit (Pierce, Rockford, IL). For Western blot, 10  $\mu\text{g}$  of protein was loaded and separated by 10% sodium dodecyl sulfate–polyacrylamide gel electrophoresis (SDS-PAGE) and then transferred for 1 h at 100 V to nitrocellulose membranes in transfer buffer (25 mM Tris HCl, 192 mM glycine, 20% methanol, pH 8.3) and blocked with 5% BSA blocking buffer for 1 h on a horizontal shaker. The blocked membranes were incubated with 1:1000 rabbit polyclonal lamin A/C (Cell Signaling Technology, Beverly, MA) antibody overnight at 4 °C followed by washing with Tris buffered saline (TBS) solution

with the detergent Tween-20 (TBST: 20 mM Tris/HCl, 150 mM NaCl, 0.1% Tween-20, pH 8.0). Then the membranes were probed with horseradish peroxidase (HRP)-labeled goat anti-rabbit secondary antibody (1:5000, Zhongshan Goldenbridge Biotechnology Company, Zhongshan, Guangdong Province, China) in 5% BSA buffer for 1 h at room temperature. The blots were developed by using an ECL kit (Pierce, Rockford, IL). At last, the membranes were exposed by using Bio-Rad UNIVERSAL HOOD II (Bio-Rad Laboratory, Bossier City, LA).

**Acknowledgment.** The authors thank National Natural Science Foundation of China (Nos. 30970784 and 30772007), National Key Basic Research Program of China (2009CB930200), Chinese Academy of Sciences (CAS) "Hundred Talents Program" (07165111ZX), China–Finland Nanotechnology (No. 2008DFA01510), Tianjin Natural Science Foundation (09JCYB-JC13800), and Tianjin University Youth Teacher Culture Foundation (TJU-YFF-08B15) for financial support.

**Supporting Information Available:** Preparation process of charge-reversal polyelectrolyte-coated gold nanoparticles using layer-by-layer technique; TEM images of colloidal AuNPs after the coating steps; fluorescence microscope image of 293T cells transfected with DNA/PEI/PAH-Cit/PEI/MUA-AuNP complexes; and cell viability of HeLa cells treated with PEI/PAH-Cit/PEI/MUA-AuNPs and nucleic acid complexes by MTT assay. This material is available free of charge via the Internet at <http://pubs.acs.org>.

## REFERENCES AND NOTES

- Prabaharan, M.; Grailer, J. J.; Pilla, S.; Steeber, D. A.; Gong, S. Q. Gold Nanoparticles with a Monolayer of Doxorubicin-Conjugated Amphiphilic Block Copolymer for Tumor-Targeted Drug Delivery. *Biomaterials* **2009**, *30*, 6065–6075.
- Gibson, J. D.; Khanal, B. P.; Zubarev, E. R. Paclitaxel-Functionalized Gold Nanoparticles. *J. Am. Chem. Soc.* **2007**, *129*, 11653–11661.
- Hong, R.; Han, G.; Fernandez, J. M.; Kim, B. J.; Forbes, N. S.; Rotello, V. M. Glutathione-Mediated Delivery and Release Using Monolayer Protected Nanoparticle Carriers. *J. Am. Chem. Soc.* **2006**, *128*, 1078–1079.
- Aryal, S.; Grailer, J. J.; Pilla, S.; Steeber, D. A.; Gong, S. Q. Doxorubicin Conjugated Gold Nanoparticles as Water-Soluble and pH-Responsive Anticancer Drug Nanocarriers. *J. Mater. Chem.* **2009**, *19*, 7879–7884.
- Kim, C. K.; Ghosh, P.; Pagliuca, C.; Zhu, Z. J.; Menichetti, S.; Rotello, V. M. Entrapment of Hydrophobic Drugs in Nanoparticle Monolayers with Efficient Release into Cancer Cells. *J. Am. Chem. Soc.* **2009**, *131*, 1360–1361.
- Ghosh, P. S.; Kim, C. K.; Han, G.; Forbes, N. S.; Rotello, V. M. Efficient Gene Delivery Vectors by Tuning the Surface Charge Density of Amino Acid-Functionalized Gold Nanoparticles. *ACS Nano* **2008**, *2*, 2213–2218.
- Thomas, M.; Klibanov, A. M. Conjugation to Gold Nanoparticles Enhances Polyethylenimine's Transfer of Plasmid DNA into Mammalian Cells. *Proc. Natl. Acad. Sci. U.S.A.* **2003**, *100*, 9138–9143.
- Rhim, W. K.; Kim, J. S.; Nam, J. M. Lipid-Gold-Nanoparticle Hybrid-Based Gene Delivery. *Small* **2008**, *4*, 1651–1655.
- Niidome, T.; Nakashima, K.; Takahashi, H.; Niidome, Y. Preparation of Primary Amine-Modified Gold Nanoparticles and Their Transfection Ability into Cultivated Cells. *Chem. Commun.* **2004**, 1978–1979.
- Lee, Y.; Miyata, K.; Oba, M.; Ishii, T.; Fukushima, S.; Han, M.; Koyama, H.; Nishiyama, N.; Kataoka, K. Charge-Conversion Ternary Polyplex with Endosome Disruption Moiety: A Technique for Efficient and Safe Gene Delivery. *Angew. Chem., Int. Ed.* **2008**, *47*, 5163–5166.
- Elbakry, A.; Zaky, A.; Liebkl, R.; Rachel, R.; Goepfertich, A.; Breunig, M. Layer-by-Layer Assembled Gold Nanoparticles for siRNA Delivery. *Nano Lett.* **2009**, *9*, 2059–2064.
- Lee, J. S.; Green, J. J.; Love, K. T.; Sunshine, J.; Langer, R.; Anderson, D. G. Gold, Poly(β-amino ester) Nanoparticles for Small Interfering RNA Delivery. *Nano Lett.* **2009**, *9*, 2402–2406.
- Giljohann, D. A.; Seferos, D. S.; Prigodich, A. E.; Patel, P. C.; Mirkin, C. A. Gene Regulation with Polyvalent siRNA–Nanoparticle Conjugates. *J. Am. Chem. Soc.* **2009**, *131*, 2072–2073.
- Han, G.; You, C. C.; Kim, B. J.; Turingan, R. S.; Forbes, N. S.; Martin, C. T.; Rotello, V. M. Light-Regulated Release of DNA and Its Delivery to Nuclei by Means of Photolabile Gold Nanoparticles. *Angew. Chem., Int. Ed.* **2006**, *45*, 3165–3169.
- Braun, G. B.; Pallaoro, A.; Wu, G.; Missirlis, D.; Zasadzinski, J. A.; Tirrell, M.; Reich, N. O. Laser-Activated Gene Silencing via Gold Nanoshell–siRNA Conjugates. *ACS Nano* **2009**, *3*, 2007–2015.
- Chen, C.-C.; Lin, Y.-P.; Wang, C.-W.; Tzeng, H.-C.; Wu, C.-H.; Chen, Y.-C.; Chen, C.-P.; Chen, L.-C.; Wu, Y.-C. DNA–Gold Nanorod Conjugates for Remote Control of Localized Gene Expression by Near Infrared Irradiation. *J. Am. Chem. Soc.* **2006**, *128*, 3709–3715.
- Huang, H.-C.; Barua, S.; Kay, D. B.; Rege, K. Simultaneous Enhancement of Photothermal Stability and Gene Delivery Efficacy of Gold Nanorods Using Polyelectrolytes. *ACS Nano* **2009**, *3*, 2941–2952.
- Reynolds, A.; Leake, D.; Boese, Q.; Scaringe, S.; Marshall, W. S.; Khvorova, A. Rational SiRNA Design for RNA Interference. *Nat. Biotechnol.* **2004**, *22*, 326–330.
- Novina, C. D.; Murray, M. F.; Dykxhoorn, D. M.; Beresford, P. J.; Riess, J.; Lee, S.-K.; Collman, R. G.; Lieberman, J.; Shankar, P.; Sharp, P. A. siRNA-Directed Inhibition of HIV-1 Infection. *Nat. Med.* **2002**, *8*, 681–686.
- Xia, H.; Mao, Q.; Paulson, H. L.; Davidson, B. L. SiRNA-Mediated Gene Silencing *In Vitro* and *In Vivo*. *Nat. Biotechnol.* **2002**, *20*, 1006–1010.
- Rosi, N. L.; Giljohann, D. A.; Thaxton, C. S.; Lytton-Jean, A. K. R.; Han, M. S.; Mirkin, C. A. Oligonucleotide-Modified Gold Nanoparticles for Intracellular Gene Regulation. *Science* **2006**, *312*, 1027–1030.
- Ghosh, P.; Han, G.; De, M.; Kim, C. K.; Rotello, V. M. Gold Nanoparticles in Delivery Applications. *Adv. Drug Delivery Rev.* **2008**, *60*, 1307–1315.
- Xu, P. S.; Van Kirk, E. A.; Zhan, Y. H.; Murdoch, W. J.; Radosz, M.; Shen, Y. Q. Targeted Charge-Reversal Nanoparticles for Nuclear Drug Delivery. *Angew. Chem., Int. Ed.* **2007**, *46*, 4999–5002.
- Rozema, D. B.; Ekenna, K.; Lewis, D. L.; Loomis, A. G.; Wolff, J. A. Endosomolysis by Masking of a Membrane-Active Agent (Emma) for Cytoplasmic Release of Macromolecules. *Bioconjugate Chem.* **2003**, *14*, 51–57.
- Miyata, K.; Oba, M.; Nakanishi, M.; Fukushima, S.; Yamasaki, Y.; Koyama, H.; Nishiyama, N.; Kataoka, K. Polyplexes from Poly(aspartamide) Bearing 1,2-Diaminoethane Side Chains Induce pH-Selective, Endosomal Membrane Destabilization with Amplified Transfection and Negligible Cytotoxicity. *J. Am. Chem. Soc.* **2008**, *130*, 16287–16294.
- Liu, X. H.; Zhang, J. T.; Lynn, D. M. Polyelectrolyte Multilayers Fabricated from 'Charge-Shifting' Anionic Polymers: A New Approach to Controlled Film Disruption and the Release of Cationic Agents from Surfaces. *Soft Matter* **2008**, *4*, 1688–1695.
- Schneider, G. F.; Subr, V.; Ulrich, K.; Decher, G. Multifunctional Cytotoxic Stealth Nanoparticles. A Model Approach with Potential for Cancer Therapy. *Nano Lett.* **2009**, *9*, 636–642.
- Sejin Son, W. J. K. Biodegradable Nanoparticles Modified by Branched Polyethylenimine for Plasmid DNA Delivery. *Biomaterials* **2010**, *31*, 133–143.
- Schneider, G.; Decher, G. Functional Core/Shell Nanoparticles via Layer-by-Layer Assembly. Investigation of the Experimental Parameters for Controlling Particle Aggregation and for Enhancing Dispersion Stability. *Langmuir* **2008**, *24*, 1778–1789.
- Shackleton, S.; Lloyd, D. J.; Jackson, S. N. J.; Evans, R.; Niermeijer, M. F.; Singh, B. M.; Schmidt, H.; Brabant, G.; Kumar, S.; Durrington, P. N.; Gregory, S.; O'Rahilly, S.; Trembath, R. C. LMNA, Encoding Lamin A/C, Is Mutated in Partial Lipodystrophy. *Nat. Genet.* **2000**, *24*, 153–156.

# Supporting Information

Figure S1. Preparation process of charge-reversal polyelectrolyte coated gold nanoparticles using layer-by-layer technique and charge-reversion facilitated siRNA release mechanism.

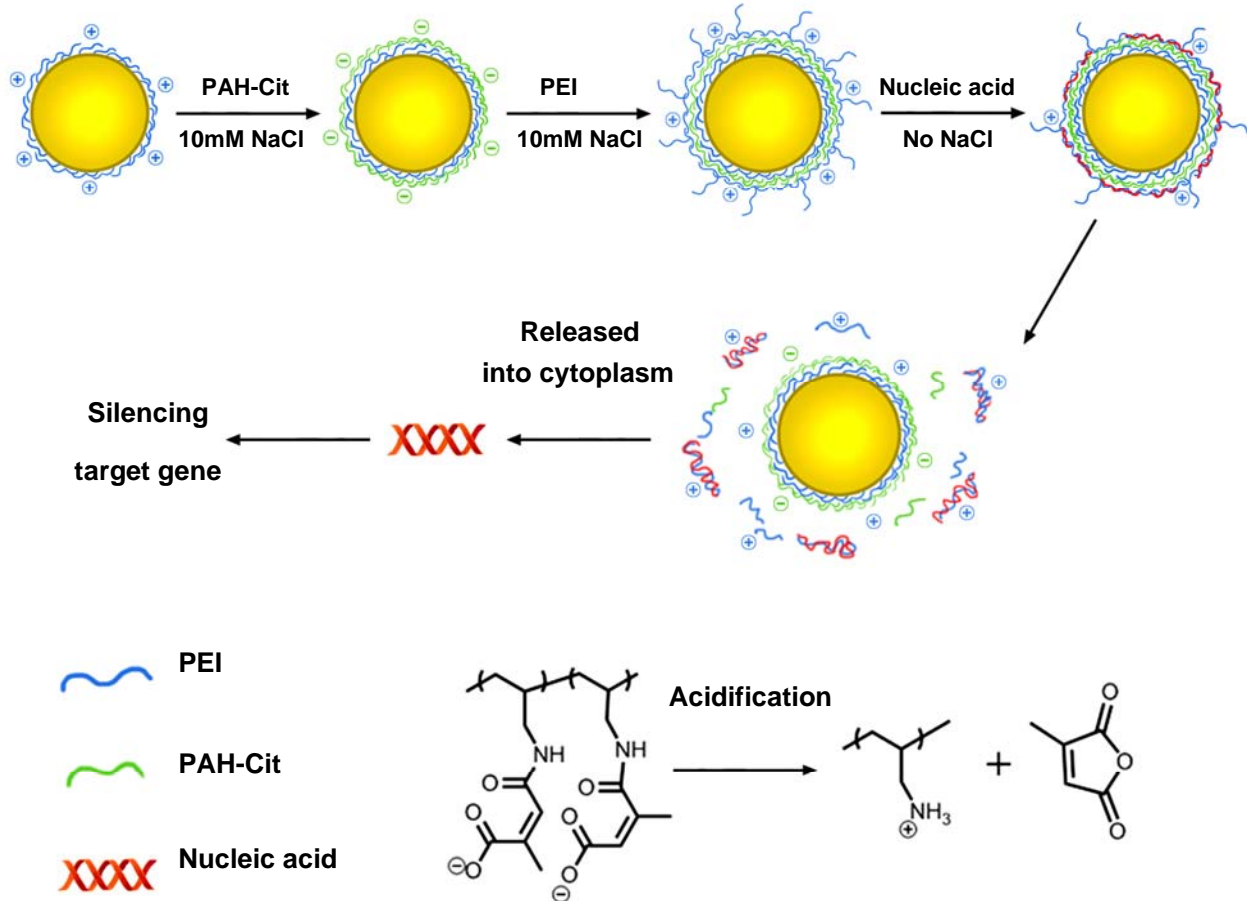


Figure S2. TEM image of colloidal Au NPs after the coating steps in 10 mM pH 7.4 HEPPS buffer.

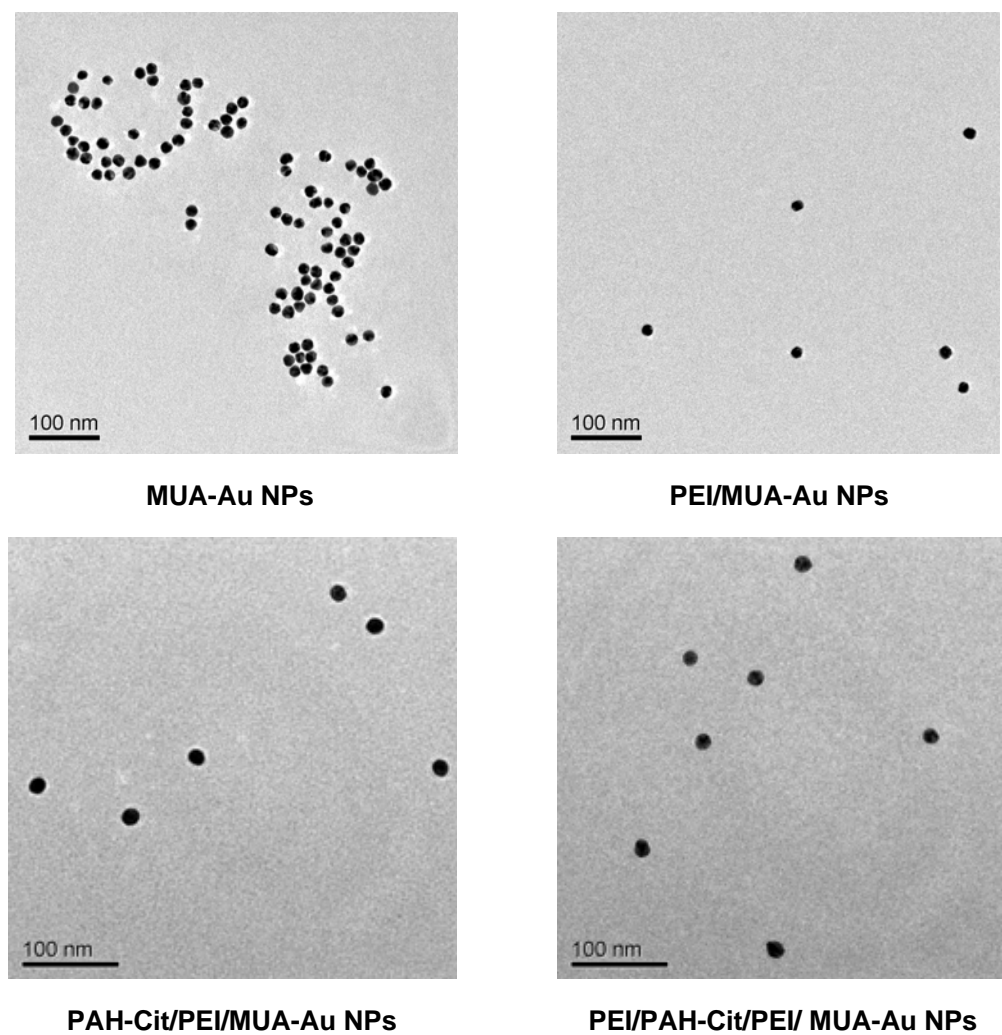


Figure S3. 293T cells transfected with DNA/PEI/PAH-Cit/PEI/MUA-Au NPs complexes and 25 kDa PEI/DNA complexes were observed by inverted fluorescence microscope. The transfection was performed at various w/w ratios of Au/DNA and PEI/DNA complexes with N/P ratio of 10 was used as control. The images were obtained at magnification of 40 $\times$ , and the bar was 30  $\mu$ m.

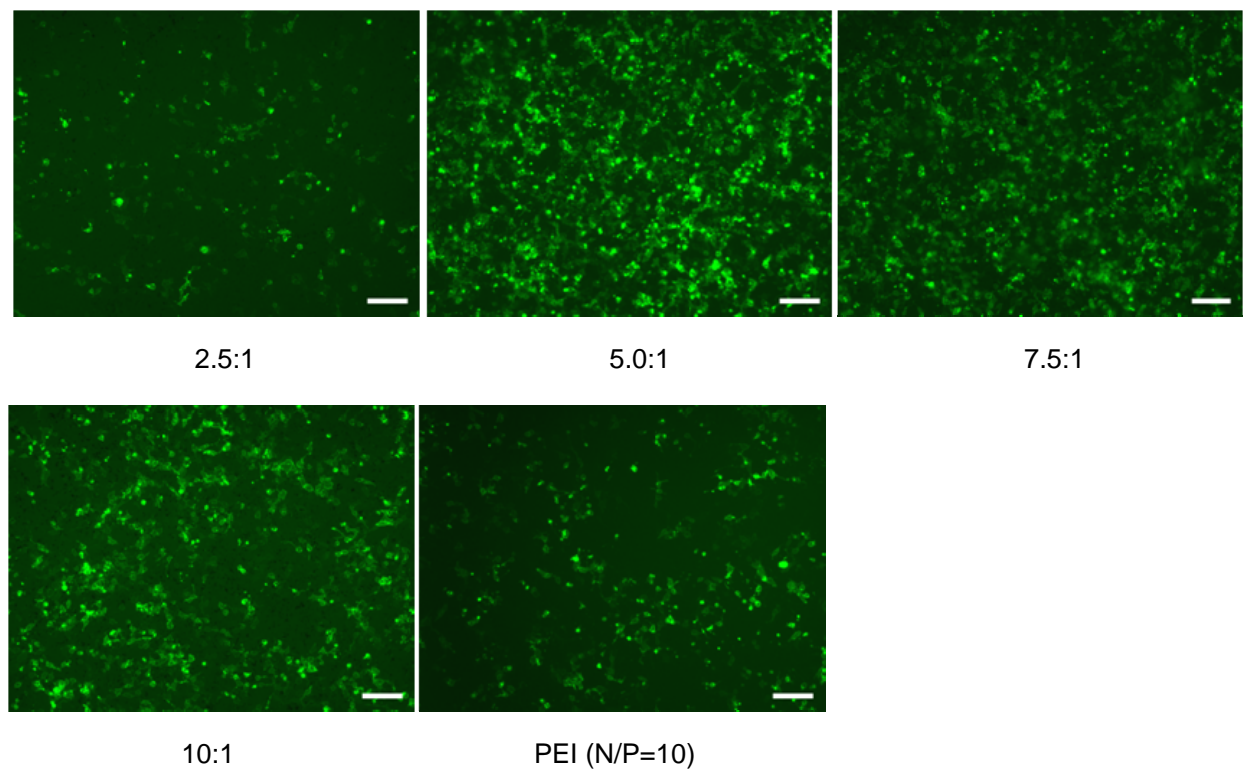


Figure S4. Cell viability of HeLa Cells treated with PEI/PAH-Cit/PEI/MUA-Au NPs/pEGFP (red) or siRNA (blue) at different w/w ratios of Au NPs to nucleic acid were determined by MTT assay. Experiments were performed in triplicate; values represent the relative viability compared to untreated cells as means  $\pm$  SEM of one representative experiment (n= 3).

